



Effective Seashell Image Classification Using CNN Algorithm

Rike Pradila¹, Yuliana Aprillia Sahuburua²
¹ Institut Teknologi Bandung, Indonesia
² Universitas Respati Yogyakarta, Indonesia

Abstract

Seashell classification presents significant challenges in image processing, particularly in distinguishing between blood shells (*Anadara granosa*) and feather mussels (*Anadara antiquata*). This study leverages deep learning and computer vision techniques to develop a classification model for seashell images using Convolutional Neural Networks (CNN). Additionally, we propose the RunCNN method to compare its performance with CNN. The research involves collecting a large dataset of blood shells and feather mussels, preprocessing the data, training the models, and evaluating their performance. Experimental results demonstrate that the CNN-based model achieves 87% accuracy, while the RunCNN method achieves 82% accuracy. Both models exhibit low loss, indicating their effectiveness in classifying seashell images. These findings highlight the potential of deep learning approaches for accurate and efficient seashell classification, with CNN outperforming RunCNN in this context.

Keywords:

Shells, CNN, RunCNN, Deep Learning

This is an open-access article under the [CC BY-SA](#) license



1. Introduction

In this study, with the advancement of digital technology in today's information age, interference in digital images has become a problem that ordinary people can solve easily. The evolution of image processing technology has both constructive and destructive aspects, especially in terms of the security of digital content. On the one hand, it shows artistic ideas and enhances the beauty of existing photos, but on the other hand, it is very easy for the enemy to destroy the content of the image in a way that is invisible to the naked eye. Classified networks were evaluated using the CASIA v2.0 dataset. Both gave an average accuracy of more than 96%, exceeding the highest result [1].

In this study, foraminifera is a microscopic single-celled sea organism (protozoa) (usually less than 1 mm) that is ubiquitous in the sea environment. During their life cycle, they build a shell out of a variety of materials, which are easily fossilized into sediments that may be extracted and studied. About 50,000 species have been listed, of which about 9,000 are nonetheless alive today. Foraminifera shells are ample in historic and contemporary-day sediments. The composition and quantity of foraminifera, as well as the chemical composition of the shells, reflect the environment in which they lived and when they became fossils, considered a record of past marine conditions. Our model is based on the Mask R-CNN architecture and uses model weight parameters learned from the COCO detection dataset [2].

In this study, mussels exhibited a complex hydrodynamic ability to filter various suspended particles from the surrounding water. As filter feeders, these krill are known to harbor disease-causing microorganisms and are therefore potentially hazardous to human

health if eaten raw or cooked. As mussels play an important role in the global fishing and aquaculture industry, supply chains selling live shellfish need to demonstrate awareness of food safety issues in the age of global trade [3].

In this study, the same shell may contain several species of worms, each represented by a variable number of metacercariae. This parasitic sub-community (i.e. the parasitic community on an individual host) differs among shellfish species by several factors, depending on the size of observations. Several studies have focused on the importance of scale in understanding the process of parasite infection, especially in intermediate hosts. At the km scale, the density of the first upstream intermediate host was the most important determinant of crustacean infectivity, whereas studies at the two scales did not show strong predictive variables. Indicates that the situation in the region is more complicated. Recently, a five-stage study, in climatic and hydrodynamic conditions, showed that the heterogeneity of large-scale ($> \times 100$ m) worms and the presence of other small-scale (10 m-1 cm) host species and migration of worms explained to become an important factor [4].

In this study, the family Cardiidae has a rich fossil record that includes 50 extant marine species and many extinct lineages. These fossils, spanning more than 215 million years old and spanning the globe, offer a unique opportunity to study the evolutionary timeline of cardids by combining many fossil calibrations to estimate the time. Divergent. In addition, ancestry ranges and ancestry patterns in ocean regions may be predicted and new geographic reconstruction methods coverage can be tested using templates, for example. Distribution-extinction-phylogenetic (DEC) model that takes into account changes in configuration plates and ocean basins over time. This study considers the complexity geographical records of this various and international population of marine bivalves, and verifies viable reasssets elucidating the relationships between contemporary marine biodiversity and major biogeographic regions of the past 135 million years. Most quoted here complete phylogenetic system so far, using multiple loci, correcting chronograms with stratigraphically delineated fossils, reconstructing the distribution of ancestry to determine the historical connection between regions and examining the overall performance of the DEC method over time concerning static geological reconstructions. And factors of the wealthy cardioid fossil record. This has a look at is the most comprehensive survey of historical biogeography based on the marine invertebrate model [5].

In this study, it should be noted that the thickness of the Li_2TiO_3 shell can easily be controlled by precisely adjusting the amount of water and washing time, offering the possibility to further optimize the overall performance of the gravel. Cross section and distribution of green gravel particles with different cleaning times. As seen in the SEM image, the green gravel has a uniform structure and there is no obvious difference between the gravels with different wash times. According to the element map, titanium concentrations are higher outdoors than indoors, which corresponds to higher indoor oxygen levels than outdoors [6].

Therefore, in this article, we provide a picture reputation version for shells using a deep learning algorithm to detect shell blood and clam feather more accurately. Our image search for images of Blood Shells and Hairy Mussels yielded the following: Contributions:

1. We have designed a brand-new category version to study shell image classification. We constructed the version that uses deep studying as opposed to the traditional classification model to identify seashell images. A high degree of accuracy and low loss rate are achieved to prove the model.
2. We evaluated our version for higher and greater picture-type consequences in the shell. It then provides a metric score chart that shows the quality of the model. In this article, we use the blood mussel and feather mussel datasets to perform experiments and create a classification model. By the usage of deep knowledge of algorithms, we can detect images on shells accurately and efficiently.
3. In our research, we can generate an accurate and efficient analysis shell image category version with the use of deep studying techniques. Instead of traditional methods, the proposed version can distinguish blood mussels & feather mussels.

2. Related Works

In this study, the tapered hull has many Engineering applications, mainly in aerospace, marine, and structural engineering. Many structures include at least some ingredients with this geometry, such as turbine blades and fuselage. These members can be subjected to dynamic stresses to varying degrees and without difficulty result in structural damage. Therefore, the detection is reliable, and the evaluation of non-destructive failures is important for the development of a system for monitoring the structural conformity of conical shell structures. The digital vibes assessment method is widely used to obtain approximate solutions for conic section shells. In some situations, such as strain sensitivity and high-frequency response, many unknown degrees of freedom must be resolved. Therefore, a new reliable method is still being developed [7].

An LSTM network combines forget-and-store mechanisms that enable the network architecture to force persistent failures in the internal state of a particular cell. These units efficiently implement non-linear mapping between input and output and feature self-adjusting and pattern recognition capabilities. Compared to other neural networks, LSTM has better approximation and error tolerance. Gyroscope body temperature data is a set of non-stationary, uneven, noisy, time-varying values and related values. The LSTM network has complex data entry requirements. Therefore, data pre-processing and hyperparameter tuning are difficult points when implementing LSTM networks [8].

In this study, the classification process was usually performed manually by separating the shells based on their shell texture. Classification is done by examining objects against the characteristics inherent in them, commonly known as attributes. Manual classification can lead to accuracy problems. Hull imaging requires the ability of structures to distinguish one hull type from another. The purpose of this research is to develop a texture feature extraction system for shell image classification. The input image is processed and segmented into an object separate from the background. The decomposed object image is converted into a grayscale image for object extraction using the local binary model method [9]. In this study, based on the experiments performed, the accuracy was very good, with the highest accuracy value occurring in the cases containing the RBF cores. The least accurate is the image test of the spring shell, with an accuracy value of 86.6%, but these results indicate that the LBP method with the SVM classification is quite reliable in calculating the accuracy of hull classification [9].

This article describes the clever design and classification system of shelled and shelled pistachios. The system includes a charger, audio components, a digital manipulator, a pneumatic rejection mechanism, and an ANN classifier. The prototype system was created to detect closed-shelled pistachios, drop them onto the steel plate, and receive the acoustic signal generated when the pistachio hits the steel plate. This detection is based on a combination of PCA and ANN impulse noise classifier. Time and frequency domain analysis of the recorded speech signal is performed to generate useful features. PCA reduces more than 99 input parameters of the ANN model because some variables are initially represented by seven principal components (PC). Offline and online modeling was performed to find the best classifier. In the offline phase, 3200 beads are practiced according to the ANN model. Different ANN topologies have been designed with different numbers of PCs in mind. The best classifier is 7-12-2. Structure [10].

In this study, the best model was selected after performing several evaluations based on the minimum mean square error (MSE), true classification level (CCR), d correlation coefficient (r). 300 closed-shell nuts, 300 open-shell nuts, and 300 split nuts were examined, and the overall error was less than 4.3%. The results show that the CCR of the thin nut obtained with this system is superior to the previous system. Further experiments were conducted to determine the systematic accuracy of classifying open-shell and closed-shell pistachios with different sizes. The test results showed superior efficiency based on the proposed approach compared to previous techniques reported in the literature or used in the field [10].

3. Proposed Method

A. Problem Definitions

In this study, CNN algorithms were used to detect n Blood shells and feather shells from a data set containing images of Blood shell and a feather shell. We propose a shell classification model using the CNN algorithm. We use a binary classifier that divides the offered into two layers (blood & feathers). This input represents a feature vector of x and has an offset. This classification is done randomly from the data to the functions using the parameters. Its position is calculated by the weight of every item inside the vector via way of means of multiplying Settings. Equation 1 can be rewritten as Equation 2. x_i is the i -th detail of vector x . The scope of this function is $[-\infty, \infty]$. Table 1 proposes a mathematical symbol of the regulator.

Table 1 Controller math symbol

Notation	Description
x	Feature vector
b	Bias
w	Parameter matrix and vector
x_i	The i -element of vector x
sgn	Output

$$f(x) = x \cdot w + b \quad (1)$$

$$f(x) = x_1 + x_1 w_2 + \dots + X_N W_N + b \quad (2)$$

$$Output = sgn(f(x)) \quad (3)$$

This regression feature generates a commonly used value to categorize genres. Use a threshold or set a limit to a specific value. So, if $f(x) > \text{Threshold}$ then access the main magnification and otherwise the $f(x)$ input goes to the second layer. A threshold method is carried out via way of means of converting the method cost to -1 the usage of the sign function (Equation 3) and 1 (Equation) as the output. Where -1 represents the first-ranked entry and the value 1 represents the second-ranked entry.

$$sgn(x) = [-1 \text{ if } x < 0, 0 \text{ if } x = 0, 1 \text{ if } x > 0] \quad (4)$$

B. Proposed Method

A popular technique for creating an image classification model is machine learning. However, manual feature engineering is expensive and tedious. Instead of the use of conventional ML, we suggest using deep learning algorithms to build learning models for image classification. Usually, researchers can generate a classification model that is suitable for the problem using DL algorithms as an answer for picture class and business objectives. To enhance the accuracy of education and testing, the surveys can use multiple parameters in the DL algorithm. B. Epoch, Regular, Optimizer [15].

In this paper, we build a new part of the last layer, a general activation function called RunCNN, by adding Gaussian factors as elements function. Instead of using the standard

activation function to train the model, we introduce the following technique of making a linear classifier blended with a distribution to optimize the usual CNN classifier. We use a gradient approach to symbolize stride length and attain minimum (local) at some point in the education phase. According to your proof training and testing results give better accuracy than the default activation function. In particular, the correct selection of the Gauss coefficient is very important to determine the performance of the NN image classifier for the shell classification problem.

The first part creates a CNN architecture with some hidden layers and hyperparameters. Instead of the use of the conventional architecture, we introduce a brand-new CNN architecture to handle the image classification activity in the shells. This technique uses supervised learning for shell image classification by analyzing various useful features. This diagram shows the CNN topology for training a classifier using the constructed features.

CNN is a type of neural network commonly used in image data. CNN can be used to detect and recognize objects in an image. In this study, we used the CNN algorithm for image classification in shells, therefore we introduce RunCNN as a new architecture consisting of neurons that have weight, bias, and activation function.

The proposed CNN uses a lot of training the model uses use gradient descent to minimize the objective function over the model parameters. The model tests parameters in the opposite direction of the desired gradient function. Using recommended CNN topologies, calculate accuracy and loss based on build and test to obtain optimal output for various input vectors. For this investigation, we take a 1D feature dataset and tune the hyperparameters accordingly. We are caring and established. An example of training with defining computations for NNs is:

Input features $x^{(i)} \in R$

Outputs $x^{(i)} \in Y(e.g. R, \{0,1\}, \{1, \dots, p\})$

Model parameters $\theta \in R^k$

Hypothesis function $h_{\theta}: R^n \rightarrow R$

Loss function $\varrho : R \times Y \rightarrow R_+$

Figure 1 In this study, we calculate the optimization problem as follows.

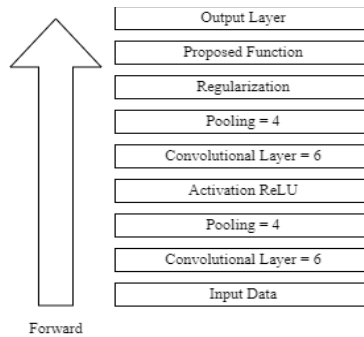


Fig. 1: RunCNN Architecture

$$\text{Minimize } \theta \sum_{i=1}^m \varrho(h_{\theta}(x^{(i)}), y^{(i)}) \quad (5)$$

This article proposes a virtual function $h_{\theta}: R^n \rightarrow R$ during neural community processing. A CNN needs to compute forward and backward sweeps to measure the slope of the model's loss function. Research on transition computation to transform An enter matrix xi with a clear out Wi produces the convolution output zi as:

$$f : R^n \rightarrow R^m \quad (6)$$

$$z_i(x_i) = W_i x_i + b \quad (7)$$

The CNN consists of a W_i filter and a bias term b which are the parameters of the convolutional layers during training. CNNs have a large number of identical neurons across layers to perform large model computations with a small number of parameters. This layer takes a single input (a feature map) and computes a feature map as output by overlapping filters of the feature map. The convolutional layer parameters are learned during training using a back-propagation model called a filter.

The second part creates a general linear activation function called a linear classifier. RunCNN and combine it using CNN models to Improve model performance. This method generates a binary classifier, which is probably the most common deep learning case. Build a train model for supervised learning by taking the input data and sending it to the hidden layer. The network to produce the output is computed with convolutional, pooling, and fully connected layers.

4. Experimental Setup

A. Main Idea

The main purpose of this work is to classify examples of blood shells and fur shells that were detected. Using the CNN algorithm. Recent advances in deep learning image processing have allowed the development of more sophisticated systems. Shell with learning technology is part of a new approach to higher accuracy. We propose a CNN based on current research with promising results in image analysis for process classification data of blood clam and feather mussels to obtain better results.

B. Dataset

For this study, we collected a dataset of seashells from Google Images and our photos including blood shell images and feathers shell images. This dataset contains training and testing with a total of 600 images. So, this data training consists of 80% of practice with 480 pictures and 20% of testing with 120 pictures. Table 2 provides approximate records of the information set used in this study.

Dataset Label	Shell Features	
	Training	Testing
Anadara Granosa	240	60
Anadara Antiquata	240	60

C. Data Preprocessing

In this study, the vectorization process was carried out. As a result, previously unstructured data must be transformed into a structured data format. Over 600 images of Blood shell and feather shell were converted using preprocessing techniques. Regional segregation, feature normalization, and feature selection. Also, since the CNN algorithm accepts image input, the sampling technique uses under-sampling and oversampling.

D. Classification Method

In this study, a training and testing process was used to create an image classification model for the pigeon & feathers shell images. Before preprocessing, the training process divides the data set into two types of data. The purpose of the preprocessing step is to

simplify the process of building classification models using CNNs. The test phase of feature extraction. Feature extraction uses 80 training vector data and 20 test vector data as training input data for process modeling using a learning process network or CNN algorithm. The community is then examined for facts validation. We then tested an effective model using test vector data to assess the model's effectiveness in classifying images of blood shells & feather shells. Finally, after going through many steps, the CNN algorithm classifies the blood shell model and the feather shell model.

5. Result and Analysis

A. Classification Test

In this study, we achieved accuracy by tuning various hyperparameters for best performance. For example, during the training and testing phase, I changed it to epochs = 25 and split validation = 0.2. In the classification process, the CNN method can be used to realize the classification model. For training, we examined datasets with three activation functions: ReLU, Sigmoid, and Tanh. We also use loss functions to estimate losses, compare losses, and measure the results of good or bad classification. Tables 3 and 4 show CNN's performance, particularly in training and testing.

To validate the RunReLU functionality on the RunCNN architecture, we compared the two classification model architectures and measured their performance during the training and testing process. In the comparison process, we placed the same hyperparameters and basic classification architectures of CNN and RunCNN on the same dataset. Tables 3, 4, 5, and 6 show the classification results using various optimization functions and the areas in between.

Table 3. Interpretation of classification results with different optimization functions and ranges between them.

CNN			
Hyperparameter	Activation Function	Accuracy	Validation Accuracy
Epoch = 25	ReLU	1.0000	0.8750
Learning Rate = 0.001	Tanh	0.4844	0.5312
Validation Split = 0.2	Sigmoid	0.4818	0.5312

Table 4. Interpretation of classification results with different optimization functions and ranges between them.

CNN			
Hyperparameter	Activation Function	Loss	Validation Loss
Epoch = 25	ReLU	0.0018	0.3377
Learning Rate = 0.001	Tanh	0.6930	0.6929
Validation Split = 0.2	Sigmoid	0.6937	0.6931

Table 3 shows the results of the accuracy of CNN model performance, especially during training and testing. ReLU, Tanh, and Sigmoid are three activation functions used to

determine model accuracy. I tested the training data using the ReLU activation function and got an accuracy of 1.0000 and a validation accuracy of 0.8750. We then tested the Tanh activation function and obtained an accuracy of 0.4844 and a validation accuracy of 0.5312. Then I tested it with the sigmoidal activation function and got 0.4818 accuracy and 0.5312 validation accuracy.

Table 4 shows the performance loss results for the CNN model with three activation functions. For the first test, we use the ReLU activation function and get a loss of 0.0018 and a validation loss of 0.3377. From the second test, the loss is 0.6930 and the validation loss is 0.6929 using Tanh. The final test of the sigmoidal activation function resulted in a loss of 0.6937 and a validation loss of 0.6931.

Table 5. Explain the classification results with various optimizer functions and the range between them.

RunCNN			
Hyperparameter	Activation Function	Accuracy	Validation Accuracy
Epoch = 25			
Learning Rate = 0.001	ReLU	1.0000	0.8229
Validation Split = 0.2			

Table 6. Explain the classification results with various optimizer functions and the range between them.

RunCNN			
Hyperparameter	Activation Function	Loss	Validation Loss
Epoch = 25			
Learning Rate = 0.001	ReLU	0.0013	0.3623
Validation Split = 0.2			

Table 5 shows the results of the RunCNN model's performance accuracy, especially during training and testing. ReLU is an activation function used to determine the accuracy of the model. I tested the training data with the ReLU activation function and got an accuracy of 1,0000 and a validation accuracy of 0.8229.

Table 6 suggests the overall performance loss consequences for the RunCNN version with the activation function. For this test, we the use ReLU activation function to obtain a loss of 0.0013 and a validation loss of 0.3623.

B. Evaluation Metric

We used the F1 score and confusion matrix to evaluate the performance of the model (CF). In this study, reminiscence is calculated to decide the proportion of records for blood shell (*Anadara Granosa*) and feather shell (*Anadara Antiquata*). Accuracy then determined the dataset levels and identified them as blood clams (*Anadara Granosa*) & feathers clams (*Anadara Antiquata*). Finally, we calculated the accuracy ratios for identifying the blood shells (*Anadara Granosa*) & feather shells (*Anadara Antiquata*) and reported low accuracy when the test results were not significant. Therefore, we need the F1 score. Optimal combination of CNN and RunCNN accuracy and coverage. Memory, accuracy, and F1 scores for the benchmark dataset are shown in Tables 7 and 8.

Table 7. Matrix Evaluation Result CNN

Classification Report	Precision	Recall	F1-Score	Support
A.Granosa	0.82	0.93	0.87	60
A.Antiquata	0.92	0.80	0.86	60
Micro avg	0.87	0.87	0.87	120
Macro avg	0.87	0.87	0.87	120
Weighted avg	0.87	0.87	0.87	120
Samples avg	0.87	0.87	0.87	120

Table 8. Matrix Evaluation Result RunCNN

Classification Report	Precision	Recall	F1-Score	Support
A.Granosa	0.79	0.87	0.83	60
A.Antiquata	0.85	0.77	0.81	60
Micro avg	0.82	0.82	0.82	120
Macro avg	0.82	0.82	0.82	120
Weighted avg	0.82	0.82	0.82	120
Samples avg	0.82	0.82	0.82	120

To ensure RunCNN performance, we also calculated a CM as a scoring metric. Figures 2 and 3 show the general CM for CNN and RunCNN.

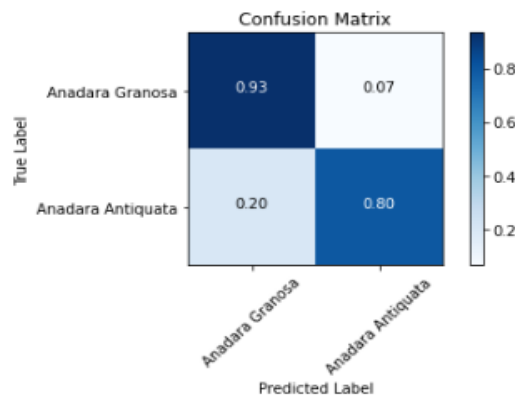


Fig 2. CM of CNN

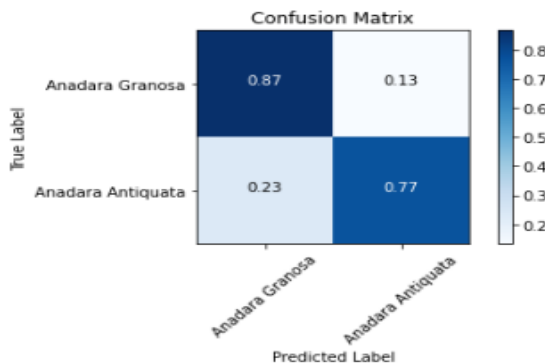


Fig 3. CM of RunCNN

Fig 2 Shows CM using the CNN algorithm for prediction values out of confusion matrices

of two distinct classes. chaos matrix score TP = 0.93, TN = 0.67, FP = 0.07, FN = 0.20. Fig. 3 displays the rating of an index with CM with the classifier's prediction values out of confusion matrices of two distinct classes. The confusion matrix is TP = 0.87, TN = 0.77, FP = 0.13, and FN = 0.23. Based on the results of the confusion matrix, the proposed version has an excessive TP rating to successfully expect wonderful data, a TN to accurately predict negative data, and a higher score for blood shell and reflects the maximum detection rate in feather shell. In particular, our approach not only provides superior accuracy but also improves graphics performance.

6. Conclusion

Shellfish are aquatic animals including mollusks. Although the definition of a mollusk is general and has no biological meaning, it is widely used and used in economic activities. Shells in the broadest sense are all mollusks with a pair of shells. In this study, we used CNN and RunCNN to build an image classification model for artillery shells while simultaneously comparing models on the image classification of the pigeon & feathers shells with the lowest possible loss for better performance and a more robust model.

From the experimental results, the best performance results are obtained by tuning the activation function which is used to optimize the model's performance. We set the epoch to 25, split the validation to 0.2, the learning rate to 0.001, and use a callback that focuses on minimal loss validation during training and testing. During training, CNN's model can produce a validation accuracy of 0.8750%, which corresponds to a validation loss of 0.3377%. And the RunCNN model can produce a validation accuracy of 0.8229%, this corresponds to a validation loss of 0.3623. Classification can be a promising solution to overcome the image classification of pigeons & feathers shells. In addition, the proposed model can obtain TP = 0.93 and TN = 0.67 for the CNN model, and TP = 0.87 and TN = 0.77 for the RunCNN model.

As a future research direction, semantic network properties can be used instead of training node information. Image clarity and sharpness are very influential in achieving greater accuracy. In addition, the R-CNN or Faster R-CNN algorithm can be used to improve the classification accuracy results.

References

- [1] S. Nath and R. Naskar, "Automated image splicing detection using deep CNN-learned features and ANN-based classifier," *Signal, Image and Video Processing*, vol. 15, pp. 1601–1608, 2021. DOI: [10.1007/s11760-021-01945-8](https://doi.org/10.1007/s11760-021-01945-8).
- [2] T. Johansen, S. A. Sørensen, K. Møllersen, and F. Godtliebsen, "Instance segmentation of microscopic foraminifera," *arXiv preprint arXiv:2105.14191*, 2021.
- [3] F. Ricardo et al., "Potential use of fatty acid profiles of the adductor muscle of cockles (*Cerastoderma edule*) for traceability of collection site," *Scientific Reports*, vol. 5, 2015. DOI: [10.1038/srep11125](https://doi.org/10.1038/srep11125).
- [4] X. Montaudouin, C. Biniyas, and G. Lassalle, "Assessing parasite community structure in cockles *Cerastoderma edule* at various spatio-temporal scales," *Estuarine, Coastal and Shelf Science*, vol. 110, pp. 54–60, 2012. DOI: [10.1016/j.ecss.2012.03.015](https://doi.org/10.1016/j.ecss.2012.03.015).
- [5] N. D. Herrera et al., "Molecular phylogenetics and historical biogeography amid shifting continents in the cockles and giant clams (*Bivalvia: Cardiidae*)," *Molecular Phylogenetics and Evolution*, vol. 93, pp. 94–106, 2015. DOI: [10.1016/j.ympev.2015.07.013](https://doi.org/10.1016/j.ympev.2015.07.013).
- [6] M. Hong, Y. Zhang, Y. Mi, M. Xiang, and Y. Zhang, "Fabrication and characterization of Li₂TiO₃ core-shell pebbles with enhanced lithium density," *Journal of Nuclear Materials*, vol. 445, pp. 111–116, 2014. DOI: [10.1016/j.inucmat.2013.10.045](https://doi.org/10.1016/j.inucmat.2013.10.045).

- [7] J. Xiang, T. Matsumoto, Y. Wang, and Z. Jiang, "Detect damages in conical shells using curvature mode shape and wavelet finite element method," *International Journal of Mechanical Sciences*, vol. 66, pp. 83–93, 2013. DOI: [10.1016/j.ijmecsci.2012.10.012](https://doi.org/10.1016/j.ijmecsci.2012.10.012).
- [8] H. Shi, "LSTM based prediction algorithm and abnormal change detection for temperature in aerospace gyroscope shell," *International Journal of Intelligent Computing and Cybernetics (IJICC)*, 2019. DOI: [10.1108/IJICC-01-2019-0001](https://doi.org/10.1108/IJICC-01-2019-0001).
- [9] P. A. R. Devi and R. P. N. Budiarti, "Image classification with shell texture feature extraction using local binary pattern (LBP) method," *Applied Technology and Computing Science Journal*, 2020.
- [10] S. Chiba, "Taxonomic revision of the fossil land snail species of the genus *Mandarina* in the Ogasawara Islands," *Paleontological Research*, 2007. DOI: [10.2517/1342-8144-11.1.1](https://doi.org/10.2517/1342-8144-11.1.1).
- [11] S. M. Keogh and A. M. Simons, "Molecules and morphology reveal 'new' widespread North American freshwater mussel species (Bivalvia: Unionidae)," *Molecular Phylogenetics and Evolution*, vol. 138, pp. 182–192, 2019. DOI: [10.1016/j.ympev.2019.05.024](https://doi.org/10.1016/j.ympev.2019.05.024).
- [12] J. G. Carter and G. R. Clark, "Classification and phylogenetic significance of molluscan shell microstructure," *Treatise on Invertebrate Paleontology*, 1985.
- [13] L. R. L. Simone, D. C. Cavallari, and R. B. Salvador, "A new troglobite species of *Habeastrum* Simone, 2019 from Brazil, and support for classification in Diplommatinidae (Mollusca, Caenogastropoda)," *Zoosystematics and Evolution*, vol. 96, pp. 639–647, 2020. DOI: [10.3897/zse.96.52868](https://doi.org/10.3897/zse.96.52868).
- [14] I. Tëmkin, "Morphological perspective on the classification and evolution of Recent Pterioidea (Mollusca: Bivalvia)," *Zoological Journal of the Linnean Society*, vol. 148, pp. 253–312, 2006. DOI: [10.1111/j.1096-3642.2006.00257.x](https://doi.org/10.1111/j.1096-3642.2006.00257.x).
- [15] E. I. Vorobyov and S. Basu, "The effect of a finite mass reservoir on the collapse of spherical isothermal clouds and the evolution of protostellar accretion," *Monthly Notices of the Royal Astronomical Society*, vol. 360, pp. 675–684, 2005. DOI: [10.1111/j.1365-2966.2005.09053.x](https://doi.org/10.1111/j.1365-2966.2005.09053.x).